Molecular convergence and positive selection associated with the evolution of symbiont transmission mode in stony corals

Groves B. Dixon[a,1] and Carly D. Kenkel[b,2]

[a]Department of Integrative Biology, The University of Texas at Austin, 1 University Station C0990, Austin, TX 78712, USA

[b]Department of Biological Sciences, University of Southern California, 3616 Trousdale Parkway, Los Angeles, CA 90089, USA

[1]Email: grovesdixon@gmail.com

[2]Corresponding author, email: ckenkel@usc.edu; phone: 213-821-1705; fax: 213-740-8123

KEYWORDS: intracellular symbiosis, *Scleractinia*, transcriptomes, molecular evolution, dN/dS

DATA ARCHIVAL LOCATION: Raw sequencing data generated for this study have been uploaded to NCBI's SRA: PRJNA395352. All bioinformatic scripts and input files can be found at https://github.com/grovesdixon/convergent_evo_coral.

Abstract

Heritable symbioses are thought to be important for the maintenance of mutually beneficial relationships (1), and for facilitating major transitions in individuality, such as the evolution of the eukaryotic cell (2, 3). In stony corals, vertical transmission has evolved repeatedly (4), providing a unique opportunity to investigate the genomic basis of this complex trait. We conducted a comparative analysis of 25 coral transcriptomes to identify orthologous genes exhibiting both signatures of positive selection and convergent amino acid substitutions in vertically transmitting lineages. The frequency of convergence events tends to be higher among vertically transmitting lineages, consistent with the proposed role of natural selection in driving the evolution of convergent transmission mode phenotypes (5). Of the 10,774 total orthologous genes identified, 403 exhibited at least one molecular convergence event and evidence of positive selection in at least one vertically transmitting lineage. Functional enrichments among these top candidate genes include processes previously implicated in mediating the coral-*Symbiodiniaceae* symbiosis including endocytosis, immune response, cytoskeletal protein binding and cytoplasmic membrane-bounded vesicles (6). We also identified 100 genes showing evidence of positive selection at the particular convergence event. Among these, we identified several novel candidate genes, highlighting the value of our approach for generating new insight into the mechanistic basis of the coral symbiosis, in addition to uncovering host mechanisms associated with the evolution of heritable symbioses.

Introduction

For organisms that engage in symbiosis, the mode in which symbionts are transmitted to the next host generation is a major factor governing the ecological and evolutionary dynamics of the relationship across multiple scales of biological organization. For example, transmission mode is known to influence genome size and content, cooperative interactions between partners, holobiont ecology, and the speciation rates of both partners (7–11). Two transmission modes predominate in nature: offspring can either directly inherit symbionts, typically through the maternal line in the process of vertical transmission, or they can horizontally acquire symbionts from the environment, usually early in their development (reviewed in (12)); although it is important to note that the mode of transmission can change over evolutionary time (13) and mixed-mode transmission is also possible (12). In microbial symbioses, horizontal transmission is the basal state and repeated transitions to vertical transmission may have arisen as a means to further promote host-symbiont cooperation (13–15). Vertical transmission has been hypothesized to play an important role in the maintenance of mutually beneficial symbioses (1), and likely facilitated major evolutionary transitions in individuality, such as the evolution of the eukaryotic cell (2, 3). From the perspective of the symbiont, the genomic consequences of evolving a heritable symbiosis include a reduction in genome size and increased dependence on their hosts due to the loss of functionally redundant genes (3, 10). However, the underlying genetic architecture facilitating evolution of a heritable symbiosis from the perspective of the host remains unresolved.

The evolution of vertical transmission is predicted to be correlated with the evolution of host control mechanisms (16) and theory predicts a high rate of mutation in genes responsible for the host-symbiont fitness interaction (17). Selection on mechanisms critical for the establishment

70 and maintenance of a horizontally transmitted symbiosis, such as cell surface molecules
71 mediating inter-partner recognition, is likely also relaxed (12). Among metazoan hosts, diverse
72 behavioral, developmental and physiological mechanisms are known to facilitate the vertical
73 transmission of microbial endosymbionts (13, 16), yet there is also some evidence for phenotypic
74 convergence. For example, plant-sucking stinkbugs and lice require microbial gut symbionts to
75 facilitate digestion of sap and blood, respectively, but both have evolved additional specialized
76 organs for housing bacteria along the female reproductive tract for the transmission of symbionts
77 to eggs (16, 18). Convergent evolution at the phenotypic level is often the result of similar
78 changes at the genomic level (19, 20) and comparative analyses have facilitated understanding of
79 the genetic basis of convergently evolved phenotypes in diverse taxa (19, 21, 22). Therefore, by
80 comparing vertically transmitting lineages with their closest horizontally transmitting relatives it
81 may be possible to identify candidate genes involved in the evolution of convergent transmission
82 mode phenotypes.

83 Reef-building corals exhibit both horizontal and vertical transmission of their obligate
84 intracellular *Symbiodiniaceae* symbionts, offering an ideal opportunity to utilize such a
85 comparative approach to identify candidate genes involved the evolution of symbiont
86 transmission mode. The majority of coral species acquire their symbionts from the environment
87 early in their development, but vertical transmission is exhibited by species in multiple different
88 lineages, indicating that transmission mode has evolved independently at least four times (4, 23).
89 Yet there is also significant morphological, physiological and ecological trait variation across the
90 coral phylogeny (24), which can confound a comparative approach. In corals, transmission mode
91 is often correlated with reproductive mode as coral species which broadcast spawn gametes tend
92 to exhibit horizontal transmission, while species that internally brood larvae largely transmit

93 symbionts vertically (4). However, the association is not perfect; some *Porites* spp. and all
94 known *Montipora* spp. have convergently evolved to broadcast spawn eggs which contain
95 *Symbiodiniaceae* (25, 26). We therefore sequenced the transcriptome of the vertically
96 transmitting broadcast spawner, *Montipora aequituberculata*, in addition to mining other
97 publicly available coral sequence resources (Table S1), to compile a set of transcriptomic
98 references in which vertical transmitters could be compared with their closest horizontally
99 transmitting relatives, while also accounting for variation in other life-history traits (Fig. 1).
100 From this dataset, we inferred orthologous groups and identified genes showing both signatures
101 of positive selection and convergent amino acid substitutions (overlapping amino acid changes
102 resulting from independent amino acid substitutions at the same position in two or more
103 lineages). We found that the frequency of molecular convergence tended to be higher among
104 vertically transmitting lineages and although top genes are enriched for biological processes
105 previously implicated in the coral-algal symbiosis, we also identify several novel candidates,
106 generating new insight into the mechanistic basis of this relationship.
107

108 **Results & Discussion**

109 *Ortholog identification*

110 To examine molecular convergence and positive selection, we compared homologous
111 coding sequences from transcriptomic data of 25 coral species. First, protein coding sequences
112 were predicted from the transcriptomic data based on open reading frames and sequence
113 homology to known proteins (27) and protein domains (28), and *FastOrtho* (29) was used to
114 assign sequences to preliminary orthologous groups (N = 106,300 groups). A subset of 1,196
115 single-copy orthologous groups with at least 20 of the 28 taxa represented was used to construct

116 a species tree (Fig. 1), which recapitulates known relationships reported in earlier studies using
117 single-gene (23, 30) and multi-gene phylogenies (31). We then identified putative single-copy
118 orthologs (groups with only a single representative sequence from each species) from the initial
119 set of 20,563 orthologous groups for which at least 7 (25%) of the species were represented. Of
120 these, 9,794 were truly single copy, whereas 10,769 had multiple sequences for one or more
121 species. Two biological explanations for this observation are gene duplication events subsequent
122 to the relevant speciation event, or transcript isoforms of the same gene (32). Transcript isoforms
123 are more likely given the nature of the dataset, but in either case, any sequence from these
124 monophyletic groupings can be appropriately compared to those from other species. Therefore,
125 rather than eliminate all orthologous groups with multiple sequences, we applied a filtering
126 approach similar to that described by (32) to retain an additional 3,298 of the 10,769 multiple
127 sequence orthologs. Specifically, we constructed gene trees from the protein alignments and
128 pruned away all but the longest of multiple sequences from single species that formed
129 monophyletic clades (Fig. S1; see Methods). In this way, we identified a total of 13,092 total
130 single copy orthologs. Orthologs were then aligned using MAFFT (33) and reverse translated
131 into codon sequences using Pal2Nal (34).
132 Orthologs were further quality filtered based on monophyly of known clades. Individual
133 gene trees were constructed from nucleotide alignments of each single-copy ortholog and
134 checked for monophyly of known clades (Fig. 1, 1-8 and Robusta/Complexa). All species fell
135 within their expected clades in 58% of the gene trees. If a single sequence fell outside of its
136 expected clade or clades, that sequence was removed and the ortholog was retained (27% of
137 orthologous groups). If more than one sequence fell outside its expected clade the ortholog was
138 removed (15% of orthologous groups). In total, this left 119,049 sequences (mean species per

139 orthologous group = 10.7) comprising 11,130 orthologous groups, hereafter referred to as genes,
140 which were used for the ancestral reconstruction and branch-site tests. Genes with fewer than 5
141 representative sequences were also removed, resulting in a final total of 10,774 genes.

142 *Evidence of positive selection and molecular convergence*

143 For each orthologous nucleotide alignment, PAML (35) was used to reconstruct the
144 ancestral amino acid at each node in the species tree and identify the amino acid changes that
145 occurred along the branches of the tree. We focused our analysis on eight clades (four with
146 vertical transmission and four with horizontal transmission), and identified all overlapping
147 substitutions, or independent substitutions occurring at the same position between the branches
148 leading directly to these clades' most recent common ancestors (Fig. 1). We classified
149 substitutions according to the type of change observed: parallel substitutions refer to the same
150 derived amino acid evolving from the same ancestral amino acid, convergent substitutions refer
151 to same derived amino acid evolving from different ancestral amino acids, divergent
152 substitutions refer to different derived amino acids evolving from the same ancestral amino acid
153 and 'all different' refer to different derived amino acids evolving from different ancestral amino
154 acids. Following (36), we consider both parallel and convergent substitutions to be indicative of
155 molecular convergence.

156 Among the vertical transmitters, we identified 8,952 amino acid positions exhibiting
157 either parallel (n=8,877) or convergent (n=75) substitutions in at least two lineages (ancestral
158 reconstruction posterior estimate > 0.8, Fig. 2A, Fig. S2). The convergence events occurred in
159 4,117 out of 10,774 total genes in the dataset, with an average of 0.71 convergent sites identified
160 per gene (median = 0; Fig. 2B). Of the four possible types of overlapping substitutions,
161 convergent substitutions were by far the least frequent (Fig. 2A; Fig. S2). The most common

162 type was divergent substitutions. The two remaining types, parallel and 'all different' occurred
163 with roughly similar frequency (Fig. 2A). Across the entire dataset, 11% of overlapping
164 substitutions were classified as molecular convergence (convergent or parallel).

165 In addition to quantifying molecular convergence, we also tested for evidence of positive
166 selection in each vertically transmitting lineage and for all vertically transmitting lineages at
167 once using the branch-site models in PAML (35). We found evidence of positive selection in
168 954 genes (LRT test FDR<0.1 in at least one branch-site test, Table S2) and many instances in
169 which molecular convergence and positive selection were detected in the same gene (Fig. 3A;
170 Fig. S3). In total, 403 genes showed at least one molecular convergence event between vertically
171 transmitting lineages as well as positive selection in at least one of the lineages (Table S3).

172 Finally, we took advantage of the fact that the branch site test identifies individual amino
173 acid positions that show evidence of positive selection (37), and identified a list of 100 genes for
174 which the particular convergence event also showed evidence of positive selection in one or both
175 lineages (branch site LRT p-value < 0.05 and BEB > 0.8; Table S4). No ontology enrichments
176 were detected for this reduced group, but annotations were recovered for 66 of the 100 genes.

177 *The frequency of molecular convergence*

178 The probability of parallel molecular evolution in response to selection is predicted to be
179 twice as high as that under neutrality (38). Enforcement of vertical transmission in a laboratory
180 manipulation of an anemone-*Symbiodiniaceae* symbiosis resulted in a host growth advantage,
181 suggesting that the evolution of vertical transmission in Cnidarian symbioses may be favored by
182 selection (39). However, an earlier analysis of genomic convergence among phenotypically
183 convergent marine mammal lineages revealed that convergence was actually highest in terrestrial
184 sister taxa in which no phenotypic convergence was evident, suggesting that the options for

185 adaptive evolution may be limited by pleiotropic constraints (22). To assess the relative
186 frequency of molecular convergence in our dataset we compared the proportion of molecular
187 convergence in overlapping substitutions among three sets of phenotype pairs (vertical
188 transmitters with other vertical transmitters, verticals with horizontals, and horizontals with other
189 horizontals). This helped to control for possible confounding factors such as differences in
190 mutation rate, and varying representation for each species based on data quality that may
191 influence the absolute levels of molecular convergence detected (40).

192 We found no significant differences among phenotypic pairings in the mean proportion of
193 molecular convergence (Fig. S4), molecular convergence and positive selection (Fig. S3), or
194 specific convergence events in which the sites were also identified as being positively selected
195 (Fig. S5). However, the proportion of convergence events is qualitatively different, and for each
196 of these three data subsets, is higher among vertically transmitting pairs (Figure S3-S5).
197 Although this pattern is tenuous, likely attributable to the small number of possible vertical-
198 vertical comparisons, it is consistent with a proposed role of natural selection in driving the
199 evolution of these convergent transmission mode phenotypes (5).

200 *Functional enrichments among top candidate genes*

201 Coral symbionts reside within host gastrodermal cells, surrounded by a host-derived
202 membrane known as the symbiosome (41). Although the specific genes mediating the
203 establishment and long-term maintenance of this relationship remain unresolved, a number of
204 biological processes are thought to be involved including host-microbe signaling, regulation of
205 the host innate immune response and cell cycle, phagocytosis, and cytoskeletal rearrangement
206 (6). To evaluate whether any of these previously highlighted processes were enriched among the
207 403 genes exhibiting both signatures of selection and convergent evolution, gene annotations

208 were obtained from comparisons against the UniProt Swiss-Prot database (27) and a categorical
209 functional enrichment analysis (FDR<0.1) was performed. Top functional enrichments
210 (FDR<0.01) among biological processes (BP) terms included regulation of developmental
211 growth and cell morphogenesis, and biological adhesion (GO:0048638; GO:0010769;
212 GO007155; GO0022610). Endocytosis (GO:0006897) and immune response (GO:0006955)
213 were also significant (FDR<0.1). Among molecular functions (MF), cytoskeletal protein binding
214 (GO:0008092) was the most significant enrichment (FDR=0.016, Fig. 3B). Extracellular region
215 (GO:0005576) was the most significantly enriched term among cellular components (CC),
216 however, this term was also highlighted in a comparison of horizontally transmitting sister clades
217 (Fig. S6), suggesting that it may be under selection in all corals and not necessarily specific to
218 the evolution of vertical transmission. Additional top CC enrichments (FDR<0.1) specific to
219 vertically transmitting lineages include cell junctions (GO:0030054) and cytoplasmic membrane-
220 bounded vesicles (GO:0016023).
221 Three individual genes, ABL proto-oncogene 1 (ABL 1, ORTHOMCL8234), filamin C
222 (ORTHOMCL8658), and poly(rC) binding protein 2 (ORTHOMCL8545), warrant additional
223 discussion as they are classified among significantly enriched GO terms in all three ontology
224 categories (BP, CC and MF) and were also among the less than 1% of genes in which the
225 particular convergence event also showed evidence of positive selection (Fig. 4; Table S4).
226 Importantly, none of these candidates have been previously implicated in the host-symbiont
227 relationship in earlier analyses focusing on either coral bleaching, the breakdown of the
228 symbiosis (42–46), or on the establishment of symbiosis in horizontally-transmitting corals (47–
229 49), highlighting the value of the present approach for identifying novel candidate genes
230 potentially underpinning the coral symbiosis.

231 ABL 1 is a ubiquitously expressed nonreceptor tyrosine kinase known to be involved in
232 organismal responses to a multitude of signals, including cell adhesion, DNA damage, oxidative
233 stress and cytokines (50). This gene that has likely evolved to serve a variety of context-
234 dependent biological functions, but is known to regulate several immune response phenotypes in
235 mammals including antigen receptor signaling in lymphocytes, and bacterial adhesion to host
236 cells (51–53). Through its role in regulating actin polymerization, ABL 1 is also involved in
237 endocytosis (54), supporting the hypothesis that it may play a key role in mediating the heritable
238 transmission of symbionts. Filamins are another family of actin-binding proteins which also
239 exhibit great functional diversity in their interactions (55). While Filamin C was not identified in
240 earlier functional genomic studies, expression of Filamin A was recently reported to be modified
241 by temperature over the course of a monthly reproductive cycle in *Pocillopora damicornis*, a
242 vertically-transmitting brooding coral (56). Similarly, Filamin B was found to be differentially
243 expressed between symbiotic and aposymbiotic *Aiptasia* anemones (57). Combined, these results
244 suggest an important role for this gene family in the maintenance and transmission of symbionts.
245 Poly(C)-binding proteins also exhibit substantial functional diversity, but they are involved in
246 transcriptional and translational regulation in addition to acting as structural components in
247 DNA-protein complexes (58). Interestingly, poly(rC) binding protein 2 is a negative regulator of
248 mitochondrial antiviral signaling protein (MAVS), a critical component of innate antiviral
249 immunity, where overexpression has been shown to reduce, and knockdown to increase, cellular
250 responses to viral infection (59). MAVS interacts with RIG-I-like (RLR) pattern recognition
251 receptors, which are located in the cytoplasm, to identify foreign RNA (60). However, they have
252 also been shown to function in defense against some bacterial pathogens (60, 61), suggesting that

253 regulation of poly(rC) binding protein 2 could be involved in suppressing host innate immune
254 responses against intracellular symbionts.
255
256 *Conclusions*

257 Climate change and other anthropogenic processes threaten corals because of the
258 sensitivity of the coral-dinoflagellate symbiosis to environmental stress (62, 63). Significant
259 work has gone into investigating the breakdown of this relationship in the process known as
260 'coral bleaching' over the past three decades, yet fundamental questions remain unresolved,
261 including a complete understanding of the genomic architecture underpinning the host-symbiont
262 relationship (6, 64). Here, rather than asking about molecular mechanisms correlated with the
263 breakdown of the coral symbiosis, we investigated a factor predicted to reinforce it: the evolution
264 of vertical symbiont transmission. While the genes identified here represent promising
265 candidates for further study, it is important to note that they likely represent only a fraction of the
266 molecular changes involved in the evolution of symbiont transmission mode as there are
267 alternate pathways to achieve the same phenotypic outcome that do not require changes at the
268 level of the coding sequence (65). Increasing genomic resources will facilitate a deeper
269 understanding of such alternative mechanisms, and the concurrent development of more
270 advanced genetic tools for manipulating the coral (66) and other Cnidarian model symbioses (67,
271 68) will facilitate quantification of the precise phenotypic effects of these novel genes, as well as
272 of changes in their sequence, contributing to a greater understanding of the cellular and
273 molecular mechanisms underpinning this specific relationship, and necessary for the evolution of
274 a heritable symbiosis.
275
276

277 **Methods**

278 *Sample preparation and sequencing for* Montipora aequituberculata *reference transcriptome*

279 Samples of *Montipora aequituberculata* were collected under the Great Barrier Reef
280 Marine Park Authority permit G12/35236.1 and G14/37318.1. To generate a *M.*
281 *aequituberculata* reference transcriptome, five replicate fragments of a single coral colony were
282 subject to a two-week temperature stress experiment as described in (5) and snap frozen samples
283 from control (27°C, days 4 and 17) and heat (31°C, days 2, 4 and 17) treatments were crushed in
284 liquid nitrogen and total RNA was extracted using an Aurum Total RNA mini kit (Bio-Rad, CA).
285 RNA quality and quantity were assessed using the NanoDrop ND-200 UV-Vis
286 Spectrophotometer (Thermo Scientific, MA) and gel electrophoresis. RNA samples from
287 replicate fragments were pooled in equal proportions and 1.8 µg was shipped on dry ice to the
288 Genome Sequencing and Analysis Facility (GSAF) at the University of Texas at Austin where
289 Illumina TruSeq Stranded libraries were prepared and sequenced on one lane of the Illumina
290 Hiseq 4000 to generate 2 x 150 PE reads.

291 *Transcriptome assembly and annotation*

292 Sequencing yielded 98 million raw PE reads. The *fastx_toolkit*
293 (http://hannonlab.cshl.edu/fastx_toolkit) was used to discard reads < 50 bp or having a
294 homopolymer run of 'A' ≥ 9 bases, retain reads with a PHRED quality of at least 20 over 80% of
295 the read and to trim TruSeq sequencing adaptors. PCR duplicates were then removed using a
296 custom perl script (https://github.com/z0on/annotatingTranscriptomes). Remaining high quality
297 filtered reads (37.7 million paired reads; 6.7 million unpaired reads) were assembled using
298 Trinity v 2.0.6 (69) using the default parameters and an *in silico* read normalization step at the
299 Texas Advanced Computing Center (TACC) at the University of Texas at Austin. Since corals

300 are ‘holobionts’ comprised of host, *Symbiodiniaceae* and other microbial components, resulting
301 assemblies were filtered to identify the host component following the protocol described in (70).
302 *Additional transcriptomic resources*
303 Transcriptomic data from 25 species of Scleractinia (stony corals) and 3 species of
304 Actiniaria (anemones) were downloaded from the web (Table S1; (71); (72); (73); (74); (75);
305 (42); (76); (77); (78); (79); (80); (81); (82); (83); (84); (70)).
306 *Protein sequence prediction*
307 To prepare sequences for protein sequence prediction, we first modified sequence
308 definition lines for each transcriptome to include the species name and an arbitrary sequence
309 number. To remove highly similar isoforms, we used cd-hit (85) to cluster sequences with a
310 sequence identity threshold of 0.98, alignment coverage for the longer sequence at least 0.3 and
311 alignment coverage of the shorter sequence at least 0.3. For each resulting cluster, we retained
312 only the longest sequence.
313 Protein coding sequences were predicted from the transcriptomic data based on open
314 reading frames and sequence homology to known proteins and protein domains. Protein
315 prediction steps were implemented with Transdecoder (86). First, the longest open reading
316 frames (ORFs) were identified using a minimum amino acid length of 100. Then protein
317 sequences were predicted from the longest ORFs based on blastp alignments against the
318 Swissprot database (27) and protein domains identified with scanHmm in HMMER version
319 3.1b2 (28). The resulting coding sequence predictions were used for all downstream analyses.
320 The predicted protein and coding sequences are available on github:
321 https://github.com/grovesdixon/transcriptomes_convergent_evo_coral.git.
322 *Ortholog assignment*

323 Predicted coding sequences were assigned to orthologous groups using FastOrtho, an
324 implementation of OrthoMCL (29) available through Pathosystems Resource Integration Center
325 (PATRIC) web resources (87)(http://enews.patricbrc.org/fastortho/). We ran FastOrtho using
326 reciprocal blastp results with an e-value cutoff of 1e-10, excluding hits with alignment lengths
327 less than 75% of subject sequences.

328 *Construction of species tree*

329 To construct a species tree, we used a subset of 1,196 single-copy orthologous groups
330 with at least 20 of the 28 taxa represented. The codon sequence alignments were concatenated in
331 phylip format for input into RAxML (88). The species tree was generated with the rapid
332 bootstrapping algorithm (100 iterations) using the GTRGAMMA model and three anemone
333 species were used as an outgroup. Trees were visualized using Dendroscope (89) and Figtree
334 http://tree.bio.ed.ac.uk/software/figtree/.

335 *Paralog pruning*

336 When putative paralogs from the same taxon were monophyletic, all but the longest
337 sequences were removed. This was done for an initial set of 20,563 orthologous groups for
338 which at least 7 (25%) of the species were represented. Protein sequences for these orthologs
339 were aligned with MAFFT using localpair (33) and gene trees were constructed using FastTree
340 (90). At this point, sequences from the three anemone species were removed, and were not used
341 for any further analyses. We used the biopython module Phylo (91) to identify gene trees for
342 which multiple sequences from single species formed monophyletic groups. Removal of these
343 sequences allowed us to include many more orthologous groups as single-copy orthologs (9,794
344 single copy orthologs prior to pruning, 13,092 after pruning). After pruning, putative single-copy
345 orthologs were reverse translated into codon sequences using Pal2Nal (34).

346 *Phylogenetic ortholog filtering*

347 Orthologous groups were further quality filtered based on monophyly of known clades.
348 Here we constructed gene trees from nucleotide alignments of each single-copy ortholog. We
349 checked these trees for monophyly of known clades (Genus *Acropora*, Genus *Montipora*, Genus
350 *Galaxia*, Genus *Porites*, favid clade with *F. scutaria* as outgroup, pocilloporid clade with *M.*
351 *auretenra* as outgroup, complex corals, robust corals), which were corroborated in our species
352 tree (Fig. 1). For 58% of gene trees, all species fell within their expected clades. If a single
353 sequence fell outside of its expected clade or clades, that sequence was removed and the ortholog
354 was retained (27% of orthologous groups). If more than one sequence fell outside its expected
355 clade, the ortholog was removed (15% of orthologous groups).

356 *Ancestral reconstruction and identification of convergent substitutions*

357 We used ancestral reconstructions to infer molecular convergence for the remaining high-
358 quality orthologous groups. For each orthologous nucleotide alignment, the ancestral amino acid
359 was identified at each node in the species tree, as well as the amino acid changes that occurred
360 along the branches of the tree. This analysis was performed with PAML (35), using the species
361 tree as a the guide. Example control files are available on the Github repository
362 (https://github.com/grovesdixon/convergent_evo_coral).

363 From the ancestral reconstruction results, we identified all substitutions that occurred at
364 the same positions in two or more selected lineages (overlapping substitutions). The selected
365 lineages included the branches leading to the common ancestor of four vertical transmitting
366 clades, and their corresponding horizontally transmitting sister clade (eight clades total, Fig. 1).
367 The horizontally transmitting sister clades were included to serve as negative controls, and for
368 normalization of GO enrichment analyses (see below). In cases where a clade was represented by

369 a single species, the terminal branch was used as the lineage for that clade (e.g. the two *Galaxia*
370 species, Fig. 1).

371 Following (36), we considered both parallel and convergent substitutions as molecular
372 convergence. For a given amino acid position, parallel substitutions refer to independent changes
373 to the same amino acid from the same ancestral amino acid. Convergent substitutions refer to
374 independent changes to the same amino acid from different ancestral amino acids. We also
375 recorded all other types of independent changes at the same site (i.e. changes to different amino
376 acids from the same ancestral amino acid, and changes to different amino acids from different
377 ancestral amino acids).

378 *Testing for evidence of positive selection*

379 We tested for evidence of positive selection using the branch-site test in PAML (35).
380 Branch-site tests were performed on each ortholog using codeml with NSsites set to 2 and fix
381 omega set to 1 for the null model, and set to 0 for the alternative model. Example command files
382 and tree files are available on Github (https://github.com/grovesdixon/convergent_evo_coral).
383 When labeling branches tested for evidence of positive selection for a given clade, only the
384 branch leading to the most recent common ancestor of the clade was labeled (Fig. S7). In other
385 words, whenever a vertically transmitting clade had more than one species, we tested for
386 evidence of positive selection in the lineage leading to the common ancestor of the clade, rather
387 than the terminal branches leading to each individual species. We made this choice because it
388 seems likely that mutations enabling a vertical transmission phenotype occurred in the lineage
389 leading to the common ancestor of the clade, in which vertical transmission was presumed to
390 have already evolved. As with the convergence analysis, in cases where a clade was represented
391 by a single species, the terminal branch for that species was labeled as foreground. Branch-site

392 tests were performed for each individual clade, and for all vertically transmitting clades at once.
393 Significance was tested using likelihood ratio tests, and p-values were adjusted to control for
394 false discovery rate using the Benjamini-Hochberg procedure (92). As with our analysis of
395 molecular convergence, we repeated the tests for the horizontally transmitting sister clades to
396 serve as a negative controls and normalization of GO enrichment. It should be noted that a
397 significant result for the branch-site test does not prove that positive selection occurred, it merely
398 provides evidence that it may have occurred. For simplicity, we refer to genes significant for
399 these tests as "positively selected" as in (22).

400 *Annotation of genes of interest*

401 Genes of interest were selected based on an overlap in both evidence of positive selection
402 and convergent substitutions. Genes were annotated based on the SwissProt database and Pfam
403 hits used for protein prediction (e-value < 1e-5, and default parameters for hmmscan). Gene
404 Ontology (GO) associations were applied to each orthologous group based on all SwissProt
405 genes used for prediction of any of its constituent sequences. The GO annotations for these genes
406 were gathered from the Gene Ontology Annotation (GOA) Database (93)
407 ftp://ftp.ebi.ac.uk/pub/databases/GO/goa/UNIPROT/). For cases when sequences in an
408 orthologous group were predicted with multiple different SwissProt hits, the orthologous group
409 was annotated with GO associations from all included SwissProt genes. Some orthologous
410 groups had only Pfam hits. These did not receive GO annotations.

411 *GO enrichment*

412 GO enrichment was performed using Fisher's exact tests on the final set of genes
413 exhibiting overlap in evidence of positive selection in at least one of the branch site tests and had
414 at least one molecular convergence event among the vertically transmitting lineages. A paired

415 control analysis was performed for genes with the same signatures among the horizontally
416 transmitting lineages (Fig. S6). To perform fewer total tests, and reduce the effect of false
417 discovery correction, only large GO terms, associated with at least 200 orthologs in our dataset,
418 were tested for enrichment.
419
420
421
422 ACKNOWLEDGEMENTS
423 This work was supported in part by an NSF International Postdoctoral Research Fellowship,
424 DBI-1401165 to CDK. Bioinformatic analyses were carried out using computational resources of
425 the Texas Advanced Computer Center (TACC).
426
427
428 STATEMENT OF AUTHORSHIP: CDK designed research and assembled new reference
429 transcriptome; GBD analyzed convergence and selection; CDK wrote the first draft of the
430 manuscript and both authors contributed to revisions.
431
432
433
434
435
436
437

438 REFERENCES

439 1. Frank SA (1996) Host-symbiont conflict over the mixing of symbiotic lineages. *Proc Biol Sci*
440 263(1368):339–344.

441 2. Kiers ET, West SA (2015) Evolving new organisms via symbiosis. *Science* 348(6233):392–
442 394.

443 3. Fisher RM, Henry LM, Cornwallis CK, Kiers ET, West SA (2017) The evolution of host-
444 symbiont dependence. *Nature Communications* 8:15973.

445 4. Hartmann AC, Baird AH, Knowlton N, Huang D (2017) The Paradox of Environmental
446 Symbiont Acquisition in Obligate Mutualisms. *Current Biology* 0(0).
447 doi:10.1016/j.cub.2017.10.036.

448 5. Kenkel CD, Bay LK (2018) Exploring mechanisms that affect coral cooperation: symbiont
449 transmission mode, cell density and community composition. *PeerJ*:in press.

450 6. Davy SK, Allemand D, Weis VM (2012) Cell Biology of Cnidarian-Dinoflagellate Symbiosis.
451 *Microbiol Mol Biol Rev* 76(2):229–261.

452 7. Herre EA, Knowlton N, Mueller UG, Rehner SA (1999) The evolution of mutualisms:
453 exploring the paths between conflict and cooperation. *Trends in Ecology & Evolution*
454 14(2):49–53.

455 8. Sauer C, Stackebrandt E, Gadau J, Hölldobler B, Gross R (2000) Systematic relationships
456 and cospeciation of bacterial endosymbionts and their carpenter ant host species:
457 proposal of the new taxon Candidatus Blochmannia gen. nov. *International Journal of*
458 *Systematic and Evolutionary Microbiology* 50(5):1877–1886.

459 9. Moran NA, Bennett GM (2014) The Tiniest Tiny Genomes. *Annual Review of Microbiology*
460 68(1):195–215.

461 10. Bennett GM, Moran NA (2015) Heritable symbiosis: The advantages and perils of an
462 evolutionary rabbit hole. *PNAS* 112(33):10169–10176.

463 11. Moran NA, McCutcheon JP, Nakabachi A (2008) Genomics and evolution of heritable
464 bacterial symbionts. *Annu Rev Genet* 42:165–190.

465 12. Bright M, Bulgheresi S (2010) A complex journey: transmission of microbial symbionts.
466 *Nature Reviews Microbiology* 8(3):218–230.

467 13. Sachs JL, Skophammer RG, Regus JU (2011) Evolutionary transitions in bacterial symbiosis.
468 *PNAS* 108(Supplement 2):10800–10807.

469 14. Sachs JL, Mueller UG, Wilcox TP, Bull JJ (2004) The Evolution of Cooperation. *The Quarterly*
470 *Review of Biology* 79(2):135–160.

471 15. West SA, Fisher RM, Gardner A, Kiers ET (2015) Major evolutionary transitions in
472 individuality. *PNAS* 112(33):10112–10119.

473 16. Frank SA (1996) Host Control of Symbiont Transmission: The Separation of Symbionts Into
474 Germ and Soma. *The American Naturalist* 148(6):1113–1124.

475 17. Drown DM, Zee PC, Brandvain Y, Wade MJ (2013) Evolution of transmission mode in
476 obligate symbionts. *Evol Ecol Res* 15(1):43–59.

477 18. Kikuchi Y, et al. (2009) Host-symbiont co-speciation and reductive genome evolution in gut
478 symbiotic bacteria of acanthosomatid stinkbugs. *BMC Biology* 7:2.

479 19. Stern DL (2013) The genetic causes of convergent evolution. *Nature Reviews Genetics*
480 14(11):751.

481 20. Conte GL, Arnegard ME, Peichel CL, Schluter D (2012) The probability of genetic parallelism
482 and convergence in natural populations. *Proc R Soc B* 279(1749):5039–5047.

483 21. Jones FC, et al. (2012) The genomic basis of adaptive evolution in threespine sticklebacks.
484 *Nature* 484(7392):55.

485 22. Foote AD, et al. (2015) Convergent evolution of the genomes of marine mammals. *Nature*
486 *Genetics* 47(3):272–275.

487 23. Kerr AM (2005) Molecular and morphological supertree of stony corals (Anthozoa:
488 Scleractinia) using matrix representation parsimony. *Biological reviews of the Cambridge*
489 *Philosophical Society* 80(4):543–558.

490 24. Madin JS, et al. (2016) The Coral Trait Database, a curated database of trait information for
491 coral species from the global oceans. *Scientific Data* 3:160017.

492 25. Fadlallah YH (1983) Sexual reproduction, development and larval biology in scleractinian
493 corals. *Coral Reefs* 2(3):129–150.

494 26. Richmond RH, Hunter CL (1990) Reproduction and recruitment of corals: comparisons
495 among the Caribbean, the Tropical Pacific, and the Red Sea. *Marine Ecology Progress*
496 *Series* 60(1/2):185–203.

497 27. Uniprot CT (2016) UniProt: the universal protein knowledgebase. *Nucleic Acids Research*
498 45(Database issue). doi:10.1093/nar/gkw1152.

499 28. Eddy SR (2011) Accelerated profile HMM searches. *PLoS Computational Biology* 7(10).
500 doi:10.1371/journal.pcbi.1002195.

501 29. Li L, Stoeckert CJJ, Roos DS (2003) OrthoMCL: Identification of Ortholog Groups for
502 Eukaryotic Genomes. *Genome Research* 13(9):2178–2189.

503 30. Kitahara M V, Cairns SD, Stolarski J, Blair D, Miller DJ (2010) A comprehensive phylogenetic
504 analysis of the Scleractinia (Cnidaria, Anthozoa) based on mitochondrial CO1 sequence
505 data. *PloS one* 5(7):e11490.

506 31. Bhattacharya D, et al. (2016) Comparative genomics explains the evolutionary success of
507 reef-forming corals. *eLife Sciences* 5:e13288.

508 32. Kocot KM, Citarella MR, Moroz LL, Halanych KM (2013) PhyloTreePruner: A phylogenetic
509 tree-based approach for selection of orthologous sequences for phylogenomics.
510 *Evolutionary Bioinformatics* 2013(9):429–435.

511 33. Katoh K, Standley DM (2013) MAFFT multiple sequence alignment software version 7:
512 Improvements in performance and usability. *Molecular Biology and Evolution* 30(4):772–
513 780.

514 34. Suyama M, Torrents D, Bork P (2006) PAL2NAL: Robust conversion of protein sequence
515 alignments into the corresponding codon alignments. *Nucleic Acids Research* 34:609–612.

516 35. Yang Z (2007) PAML 4: Phylogenetic analysis by maximum likelihood. *Molecular Biology*
517 *and Evolution* 24(Ml):1586–1591.

518 36. Zou Z, Zhang J (2015) Are convergent and parallel amino acid substitutions in protein
519 evolution more prevalent than neutral expectations? *Molecular Biology and Evolution*
520 32(8):2085–2096.

521 37. Yang Z, Wong WSW, Nielsen R (2005) Bayes empirical bayes inference of amino acid sites
522 under positive selection. *Mol Biol Evol* 22(4):1107–1118.

523 38. Orr HA (2005) The Probability of Parallel Evolution. *Evolution* 59(1):216–220.

524 39. Sachs JL, Wilcox TP (2006) A shift to parasitism in the jellyfish symbiont Symbiodinium
525 microadriaticum. *Proceedings of the Royal Society of London B: Biological Sciences*
526 273(1585):425–429.

527 40. Thomas GWC, Hahn MW (2015) Determining the Null Model for Detecting Adaptive
528 Convergence from Genomic Data: A Case Study using Echolocating Mammals. *Mol Biol*
529 *Evol* 32(5):1232–1236.

530 41. Wakefield T, Farmer M, Kempf S (2000) Revised description of the fine structure of in situ
531 "zooxanthellae" genus Symbiodinium. *The Biological Bulletin* 199(1):76–84.

532 42. Barshis DJ, et al. (2013) Genomic basis for coral resilience to climate change. *Proceedings*
533 *of the National Academy of Sciences of the United States of America* 110(4):1387–92.

534 43. Desalvo MK, et al. (2008) Differential gene expression during thermal stress and bleaching
535 in the Caribbean coral Montastraea faveolata. *Molecular Ecology* 17(17):3952–3971.

536 44. DeSalvo MK, Sunagawa S, Voolstra CR, Medina M (2010) Transcriptomic responses to heat
537 stress and bleaching in the elkhorn coral Acropora palmata. *Marine Ecology Progress*
538 *Series* 402:97–113.

539 45. Maor-Landaw K, et al. (2014) Gene expression profiles during short-term heat stress in the
540 red sea coral Stylophora pistillata. *Global Change Biology* 20(10):3026–3035.

541 46. Rodriguez-Lanetty M, Harii S, Hoegh-Guldberg O (2009) Early molecular responses of coral
542 larvae to hyperthermal stress. *Molecular Ecology* 18(24):5101–5114.

543 47. Voolstra CR, et al. (2009) The host transcriptome remains unaltered during the
544 establishment of coral–algal symbioses. *Molecular Ecology* 18(9):1823–1833.

545 48. Schnitzler CE, Weis VM (2010) Coral larvae exhibit few measurable transcriptional changes
546 during the onset of coral-dinoflagellate endosymbiosis. *Mar Genomics* 3(2):107–116.

547 49. Mohamed AR, et al. (2016) The transcriptomic response of the coral Acropora digitifera to
548 a competent Symbiodinium strain: the symbiosome as an arrested early phagosome. *Mol*
549 *Ecol* 25(13):3127–3141.

550 50. Wang JYJ (2014) The Capable ABL: What Is Its Biological Function? *Molecular and Cellular*
551 *Biology* 34(7):1188–1197.

552 51. Arce KP de, et al. (2010) Synaptic Clustering of PSD-95 Is Regulated by c-Abl through
553 Tyrosine Phosphorylation. *J Neurosci* 30(10):3728–3738.

554 52. Swimm A, et al. (2004) Enteropathogenic Escherichia coli Use Redundant Tyrosine Kinases
555 to Form Actin Pedestals. *MBoC* 15(8):3520–3529.

556 53. Huang Y, et al. (2008) The c-Abl tyrosine kinase regulates actin remodeling at the immune
557 synapse. *Blood* 112(1):111–119.

558 54. Tanos B, Pendergast AM (2006) Abl Tyrosine Kinase Regulates Endocytosis of the
559 Epidermal Growth Factor Receptor. *J Biol Chem* 281(43):32714–32723.

560 55. Feng Y, Walsh CA (2004) The many faces of filamin: A versatile molecular scaffold for cell
561 motility and signalling. *Nature Cell Biology* 6(11):1034–1038.

562 56. Crowder CM, Meyer E, Fan T-Y, Weis VM (2017) Impacts of temperature and lunar day on
563 gene expression profiles during a monthly reproductive cycle in the brooding coral
564 Pocillopora damicornis. *Molecular Ecology* 26(15):3913–3925.

565 57. Lehnert EM, et al. (2014) Extensive Differences in Gene Expression Between Symbiotic and
566 Aposymbiotic Cnidarians. *G3: Genes, Genomes, Genetics* 4(2):277–295.

567 58. Makeyev AV, Liebhaber SA (2002) The poly(C)-binding proteins: a multiplicity of functions
568 and a search for mechanisms. *RNA* 8(3):265–278.

569 59. You F, et al. (2009) PCBP2 mediates degradation of the adaptor MAVS via the HECT
570 ubiquitin ligase AIP4. *Nature Immunology* 10(12):1300–1308.

571 60. Brubaker SW, Bonham KS, Zanoni I, Kagan JC (2015) Innate Immune Pattern Recognition: A
572 Cell Biological Perspective. *Annu Rev Immunol* 33:257–290.

573 61. Chiu Y-H, Macmillan JB, Chen ZJ (2009) RNA polymerase III detects cytosolic DNA and
574 induces type I interferons through the RIG-I pathway. *Cell* 138(3):576–591.

575 62. Hughes TP, et al. (2003) Climate Change, Human Impacts, and the Resilience of Coral
576 Reefs. *Science* 301(5635):929–933.

577 63. Hoegh-Guldberg O, et al. (2007) Coral Reefs Under Rapid Climate Change and Ocean
578 Acidification. *Science* 318(5857):1737–1742.

579 64. Edmunds PJ, Gates RD (2003) Has Coral Bleaching Delayed Our Understanding of
580 Fundamental Aspects of Coral–Dinoflagellate Symbioses? *BioScience* 53(10):976–980.

581 65. Prud'homme B, Gompel N, Carroll SB (2007) Emerging principles of regulatory evolution.
582 *PNAS* 104(suppl 1):8605–8612.

583 66. Cleves PA, Strader ME, Bay LK, Pringle JR, Matz MV (2018) CRISPR/Cas9-mediated genome
584 editing in a reef-building coral. *PNAS* 115(20):5235–5240.

585 67. Jones VAS, Bucher M, Hambleton EA, Guse A (2018) Microinjection to deliver protein,
586 mRNA, and DNA into zygotes of the cnidarian endosymbiosis model Aiptasia sp. *Scientific*
587 *Reports* 8(1):16437.

588 68. Ohdera AH, et al. (2018) Upside-Down but Headed in the Right Direction: Review of the
589 Highly Versatile Cassiopea xamachana System. *Front Ecol Evol* 6.
590 doi:10.3389/fevo.2018.00035.

591 69. Grabherr MG, et al. (2011) Trinity: reconstructing a full-length transcriptome without a
592 genome from RNA-Seq data. *Nat Biotechnol* 29(7):644–652.

593 70. Kenkel CD, Bay LK (2017) Novel transcriptome resources for three scleractinian coral
594 species from the Indo-Pacific. *GigaScience* 6(9):1–4.

595 71. Polato NR, Vera JC, Baums IB (2011) Gene discovery in the threatened elkhorn coral: 454
596 sequencing of the acropora palmata transcriptome. *PLoS ONE* 6(12):e28634.

597 72. Shinzato C, et al. (2011) Using the Acropora digitifera genome to understand coral
598 responses to environmental change. *Nature* 476(7360):320–3.

599 73. Traylor-Knowles N, et al. (2011) Production of a reference transcriptome and
600 transcriptomic database (PocilloporaBase) for the cauliflower coral, Pocillopora
601 damicornis. *BMC Genomics* 12(1):585.

602 74. Lehnert EM, Burriesci MS, Pringle JR (2012) Developing the anemone Aiptasia as a
603 tractable model for cnidarian-dinoflagellate symbiosis: the transcriptome of aposymbiotic
604 A. pallida. *BMC genomics* 13:271.

605 75. Moya A, et al. (2012) Whole transcriptome analysis of the coral Acropora millepora reveals
606 complex responses to CO_2-driven acidification during the initiation of calcification.
607 *Molecular ecology* 21(10):2440–54.

608 76. Kenkel CD, Meyer E, Matz M V (2013) Gene expression under chronic heat stress in
609 populations of the mustard hill coral (Porites astreoides) from different thermal
610 environments. *Molecular ecology* 22(16):4322–34.

611 77. Libro S, Kaluziak ST, Vollmer S V. (2013) RNA-seq profiles of immune related genes in the
612 staghorn coral Acropora cervicornis Infected with white band disease. *PLoS ONE* 8(11):1–
613 11.

614 78. Sun J, Chen Q, Lun JCY, Xu J, Qiu JW (2013) PcarnBase: Development of a Transcriptomic
615 Database for the Brain Coral Platygyra carnosus. *Marine Biotechnology* 15:244–251.

616 79. Maor-Landaw K, et al. (2014) Gene expression profiles during short-term heat stress in the
617 red sea coral Stylophora pistillata. *Global Change Biology* 20:3026–3035.

618 80. Nordberg H, et al. (2014) The genome portal of the Department of Energy Joint Genome
619 Institute: 2014 updates. *Nucleic Acids Research* 42(November 2013):26–31.

620 81. Shinzato C, Inoue M, Kusakabe M (2014) A snapshot of a coral "holobiont": A
621 transcriptome assembly of the scleractinian coral, Porites, captures a wide variety of genes
622 from both the host and symbiotic zooxanthellae. *PLoS ONE* 9(1).
623 doi:10.1371/journal.pone.0085182.

624 82. Kitchen SA, Crowder CM, Poole AZ, Weis VM, Meyer E (2015) De novo assembly and
625 characterization of four anthozoan (phylum Cnidaria) transcriptomes. *G3 Genes Genomes*
626 *Genetics* 5(11):2441–2452.

627 83. Anderson DA, Walz ME, Weil E, Tonellato P, Smith MC (2016) RNA-Seq of the Caribbean
628 reef-building coral *Orbicella faveolata* (Scleractinia-Merulinidae) under bleaching and
629 disease stress expands models of coral innate immunity. *PeerJ* 4:e1616.

630 84. Davies SW, Marchetti A, Ries JB, Castillo KD (2016) Thermal and pCO2 stress elicit
631 divergent transcriptomic responses in a resilient coral. *Frontiers in Marine Science* 3:Article
632 122.

633 85. Li W, Godzik A (2006) Cd-hit: A fast program for clustering and comparing large sets of
634 protein or nucleotide sequences. *Bioinformatics* 22(13):1658–1659.

635 86. Haas BJ, et al. (2013) De novo transcript sequence reconstruction from RNA-seq using the
636 Trinity platform for reference generation and analysis. *Nature Protocols* 8(8):1494–1512.

637 87. Wattam AR, et al. (2014) PATRIC, the bacterial bioinformatics database and analysis
638 resource. *Nucleic Acids Research* 42(Database issue):581–591.

639 88. Stamatakis A (2014) RAxML version 8: A tool for phylogenetic analysis and post-analysis of
640 large phylogenies. *Bioinformatics* 30:1312–1313.

641 89. Huson DH, Scornavacca C (2012) Dendroscope 3: An interactive tool for rooted
642 phylogenetic trees and networks. *Systematic Biology* 61(6):1061–1067.

643 90. Price MN, Dehal PS, Arkin AP (2009) Fasttree: Computing large minimum evolution trees
644 with profiles instead of a distance matrix. *Molecular Biology and Evolution* 26(7):1641–
645 1650.

646 91. Talevich E, Invergo BM, Cock PJ, Chapman B a (2012) Bio.Phylo: A unified toolkit for
647 processing, analyzing and visualizing phylogenetic trees in Biopython. *BMC Bioinformatics*
648 13:209.

649 92. Benjamini Y, Hochberg Y (1995) Controlling the False Discovery Rate: a Practical and
650 Powerful Approach to Multiple Testing. *Journal of the Royal Statistical Society* 57(1):289–
651 300.

652 93. Huntley RP, et al. (2015) The GOA database: Gene Ontology annotation updates for 2015.
653 *Nucleic Acids Research* 43(D1):D1057–D1063.

654 94. Kerr AM, Baird AH, Hughes TP (2011) Correlated evolution of sex and reproductive mode
655 in corals (Anthozoa: Scleractinia). *Proceedings of the Royal Society of London B: Biological*
656 *Sciences* 278(1702):75–81.

657

658

659

660

661

662 FIGURES & FIGURE LEGENDS

663

664 Figure 1. Species tree with phenotypic labels indicating transmission mode, reproductive mode
665 and sexual system (4, 26, 94). Vertically transmitting species are indicated by filled circles at
666 their terminal nodes, horizontally transmitting species with open circles at their terminal nodes.
667 For each clade (1-8), the particular branch examined for convergent substitutions and positive
668 selection is indicated by a green highlight. In each case, this is the branch leading the common
669 ancestor of the clade. Shaded clades were considered when describing overlapping convergence
670 events, referred to as (1) Sister *Montipora*, (2) *Montipora*, (3) Sister *Galaxia*, (4) *Galaxia*, (5)
671 *Porites*, (6) Sister *Porites*, (7) Sister Pocilloporid, (8) Pocilloporid.
672

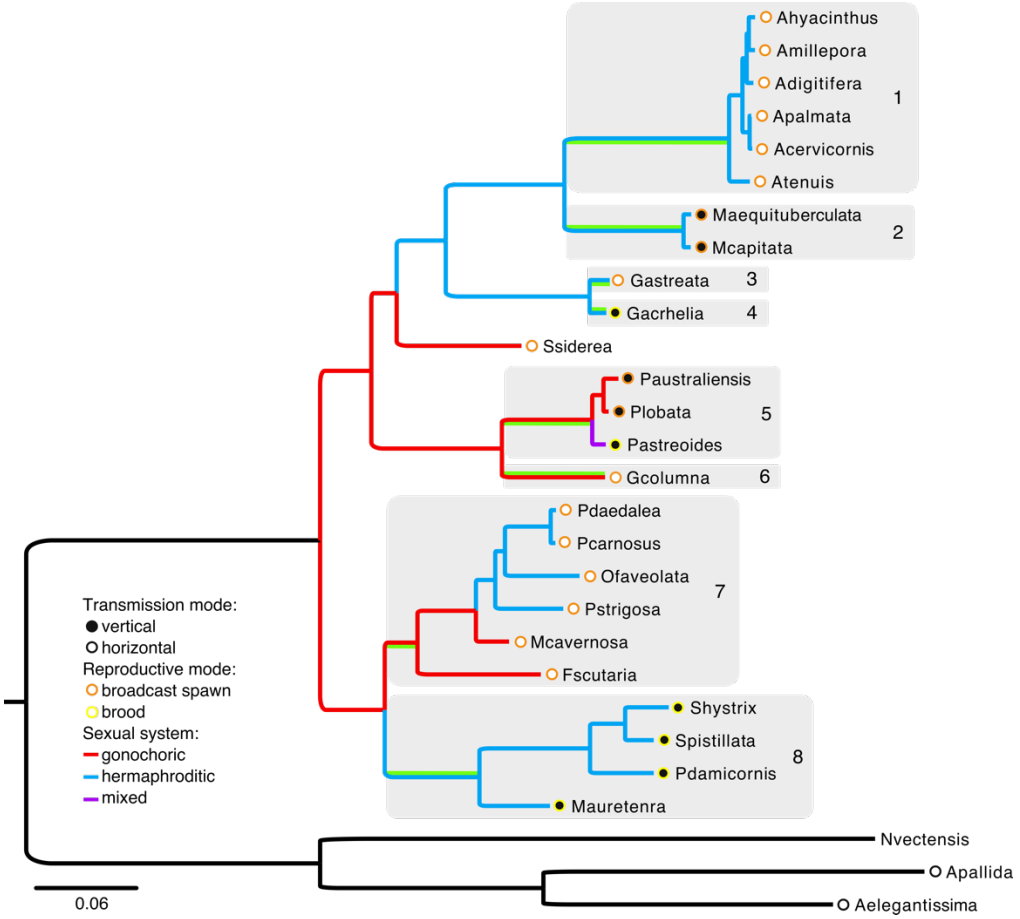

673
674
675
676
677
678
679
680
681
682

683 Figure 2. Frequency of convergence events. (A) An overlapping substitution is defined as an
684 inferred amino acid change that occurred at the same position independently in the lineages
685 leading to the common ancestor of the two indicated vertically transmitting clades. Each
686 overlapping substitution was classified into one of four categories: convergent substitutions
687 (least frequent; salmon) are changes from different amino acids to the same amino acid; parallel
688 substitutions (second most frequent; green) are changes from the same amino acid to the same
689 new amino acid; divergent substitutions (most common; teal) are changes from the same amino
690 acid to a different one; 'all different' substitutions (third most common; purple) are changes from
691 different amino acids to different new amino acids. (B) Histogram of the number of sites
692 showing molecular convergence (convergent or parallel substitutions) per tested gene (mean =
693 0.71; median=0).
694

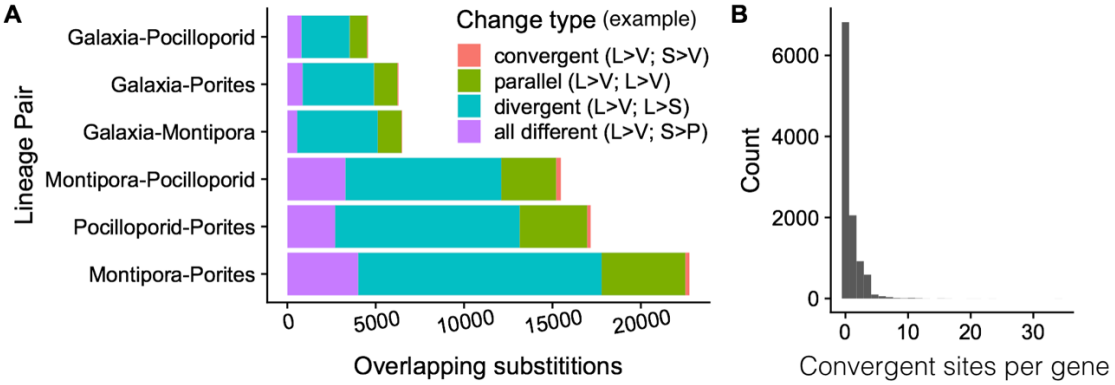

695
696
697 Figure 3. Frequency of genes exhibiting overlap in convergence and positive selection, and
698 results of a categorical functional enrichment analysis of these candidates. (A) Frequency of
699 genes exhibiting both signatures of convergence and positive selection per pair of vertically
700 transmitting clades. Black shading indicates the set of genes with at least one convergence event
701 and evidence of positive selection (FDR < 0.1) in at least one of the indicated lineages. (B) Gene
702 ontology enrichment across all convergent and positively selected genes identified for any pair of
703 vertically transmitting clades relative to the global gene list. Significance level is indicated by
704 bolded text. (BP) Biological Processes, (CC) Cellular Component, (MF) Molecular Function.
705

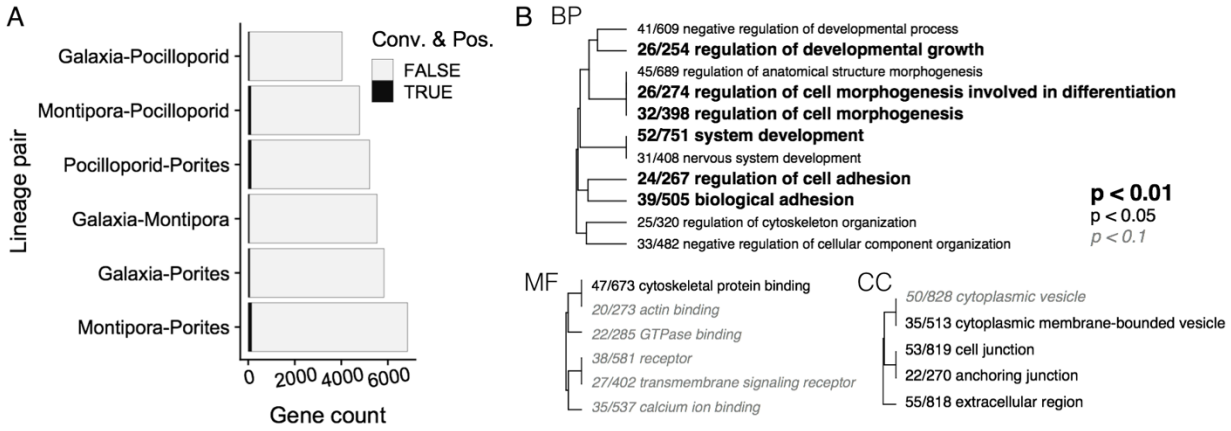

706
707

708 Figure 4. Select genes showing molecular convergence and positive selection at the same site.
709 Left panels show gene trees constructed from nucleotides for each gene. Molecular convergence
710 events that also showed evidence of positive selection are indicated with vertical bars. Tables
711 show details of the molecular convergence events and evidence of positive selection: (Pos)
712 amino acid position of convergence event; (Vert.1) first vertical lineage; (Vert. 2) second vertical
713 lineage; (Anc.1) Ancestral amino acid for first vertical lineage; (Anc.2) Ancestral amino acid for
714 second vertical lineage; (Sub.1) derived amino acid for first vertical lineage; (Sub.2) derived
715 amino acid for second vertical lineage; (BEB all) Bayes Empirical Bayes posterior probability
716 for positive selection at the position for the branch site test including all vertical transmitting
717 lineages as foreground. Derived amino acids with BEB posteriors > 0.8 for tests using individual
718 lineages as foreground are indicated with asterisks.

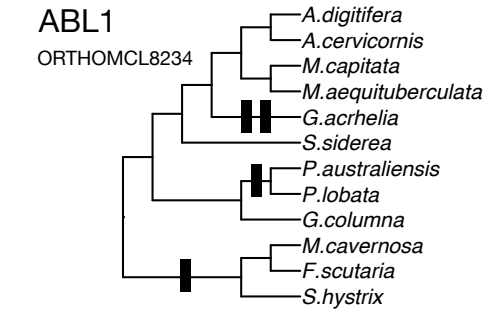

Pos	Vert.1	Vert.2	Anc.1	Anc.2	Sub.1	Sub.2	BEB all
479	Galaxia	Pocilloporid	P	P	S	S	0.98
500	Galaxia	Porites	L	L	V	V	0.84

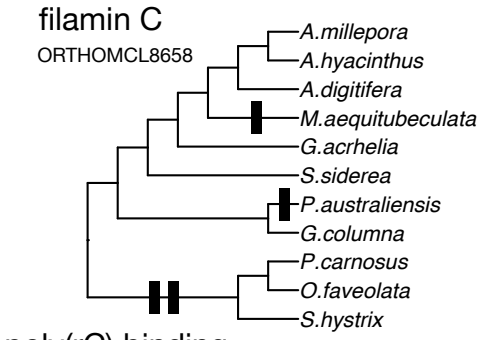

Pos	Vert.1	Vert.2	Anc.1	Anc.2	Sub.1	Sub.2	BEB all
1518	Porites	Pocilloporid	D	D	P*	P*	0.99
1973	Montipora	Pocilloporid	K	K	S	S*	0.96

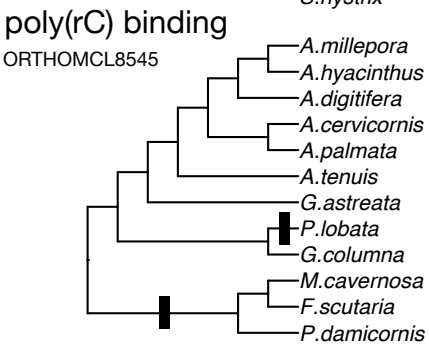

Pos	Vert.1	Vert.2	Anc.1	Anc.2	Sub.1	Sub.2	BEB all
193	Porites	Pocilloporid	K	K	S	S	0.94

719

720

721

722

723

724 SUPPLEMENTARY MATERIAL

725 Table S1. Sources of reference transcriptomes used for each species.

order	family	Genus	species	Citation	URL
Actiniaria	Actiniidae	*Anthopleura*	*elegantissima*	Kitchen et al. 2015	http://people.oregonstate.edu/~meyere/data.html
Actiniaria	Aiptasiidae	*Aiptasia*	*pallida*	Lehnert et al. 2012	http://pringlelab.stanford.edu/project%20files/AposymbioticAiptasiaTranscriptomeGoodLoci.fa.gz
Actiniaria	Edwardsiidae	*Nematostella*	*vectensis*	Nordberg et al. 2014	http://genome.jgi-psf.org/Nemve1/Nemve1.download.ftp.html
Scleractinia	Acroporidae	*Acropora*	*cervicornis*	Libro et al. 2013	http://www.ncbi.nlm.nih.gov/nuccore?LinkName=bioproject_nuccore&from_uid=222758
Scleractinia	Acroporidae	*Acropora*	*palmata*	Polato et al. 2011	http://www.personal.psu.edu/ibb3/Research.htm#Data
Scleractinia	Acroporidae	*Acropora*	*hyacinthus*	Barshis et al. 2013	http://palumbi.stanford.edu/data/
Scleractinia	Acroporidae	*Acropora*	*tenuis*	none	http://www.bio.utexas.edu/research/matz_lab/matzlab/Data_files/aten_july2014.zip
Scleractinia	Acroporidae	*Acropora*	*millepora*	Moya et al. 2012	http://www.bio.utexas.edu/research/matz_lab/matzlab/Data_files/amil_july2014.zip
Scleractinia	Acroporidae	*Acropora*	*digitifera*	Shinzato et al. 2011	http://marinegenomics.oist.jp/genomes/downloads?project_id=3
Scleractinia	Astocoeniidae	*Madracis*	*auretenra*	none	http://people.oregonstate.edu/~meyere/data.html
Scleractinia	Faviidae	*Platygyra*	*carnosus*	Sun et al. 2013	http://www.comp.hkbu.edu.hk/~db/PcarnBase/
Scleractinia	Faviidae	*Platygyra*	*daedalea*	none	http://people.oregonstate.edu/~meyere/data.html
Scleractinia	Fungiidae	*Fungia*	*scutaria*	Kitchen et al. 2015	http://people.oregonstate.edu/~meyere/data.html
Scleractinia	Merulinidae	*Orbicella*	*faveolata*	Anderson et al. 2016	https://peerj.com/articles/1616/#supplemental-information
Scleractinia	Montastraeidae	*Montastraea*	*cavernosa*	Kitchen et al. 2015	http://people.oregonstate.edu/~meyere/data.html
Scleractinia	Mussidae	*Pseudodiploria*	*strigosa*	none	http://people.oregonstate.edu/~meyere/data.html
Scleractinia	Pocilloporidae	*Pocillopora*	*damicornis*	Traylor-Knowles et al. 2011	http://cnidarians.bu.edu/PocilloporaBase/cgi-bin/pdamdata.cgi
Scleractinia	Pocilloporidae	*Seriatopora*	*hystrix*	Kitchen et al. 2015	http://people.oregonstate.edu/~meyere/data.html
Scleractinia	Pocilloporidae	*Stylophora*	*pistillata*	Maor-Landaw et al. 2014	http://data.centrescientifique.mc/Data/
Scleractinia	Poritidae	*Porites*	*astreoides*	Kenkel et al. 2013	http://www.bio.utexas.edu/research/matz_lab/matzlab/Data_files/pastreoides_may2014.zip
Scleractinia	Poritidae	*Porites*	*lobata*	none	https://www.ncbi.nlm.nih.gov/bioproject/356802
Scleractinia	Poritidae	*Porites*	*australiensis*	Shinzato et al. 2014	https://www.ncbi.nlm.nih.gov/nuccore?term=236717%5BBioProject%5D
Scleractinia	Acroporidae	*Montipora*	*aequituberculata*	none	https://www.dropbox.com/s/qvq3kus89aflyxf/Maqe.tar.gz?dl=0
Scleractinia	Acroporidae	*Montipora*	*capitata*	Frazier et al. 2017	ftp://ftp.ncbi.nlm.nih.gov/geo/series/GSE97nnn/GSE97888/suppl/GSE97888_Montiporacapitata_transcriptome.fasta.gz
Scleractinia	Oculinidae	*Galaxea*	*acrhelia*	Kenkel and Bay 2017	http://dornsife.usc.edu/labs/carlslab/data/
Scleractinia	Oculinidae	*Galaxea*	*astreata*	Kenkel and Bay 2017	http://dornsife.usc.edu/labs/carlslab/data/
Scleractinia	Poritidae	*Goniopora*	*columna*	Kenkel and Bay 2017	http://dornsife.usc.edu/labs/carlslab/data/
Scleractinia	Siderastreidae	*Siderastrea*	*siderea*	Davies et al. 2016	https://sarahwdavies.wordpress.com/data/

726

727 Figure S1: Examples of gene trees constructed for orthologous groups before and after paralog
728 pruning. Paralog pruning was performed to remove duplicate sequences from orthologous groups
729 if they came from a single species and formed a monophyletic clade. The figure shows gene trees
730 for two different orthologous groups before and after pruning. Duplicated sequences from single
731 species are shown in red. In the left orthologous group (ORTHMCL7233) a single duplicated
732 sequence from *Galaxia acrhelia* was removed. The longer of the two sequences
733 (Gacrhelia_16231.p1) was retained. In the right orthologous group, duplicate sequences formed
734 monophyletic clades six species. In each of these cases, only the longest sequence was retained.
735

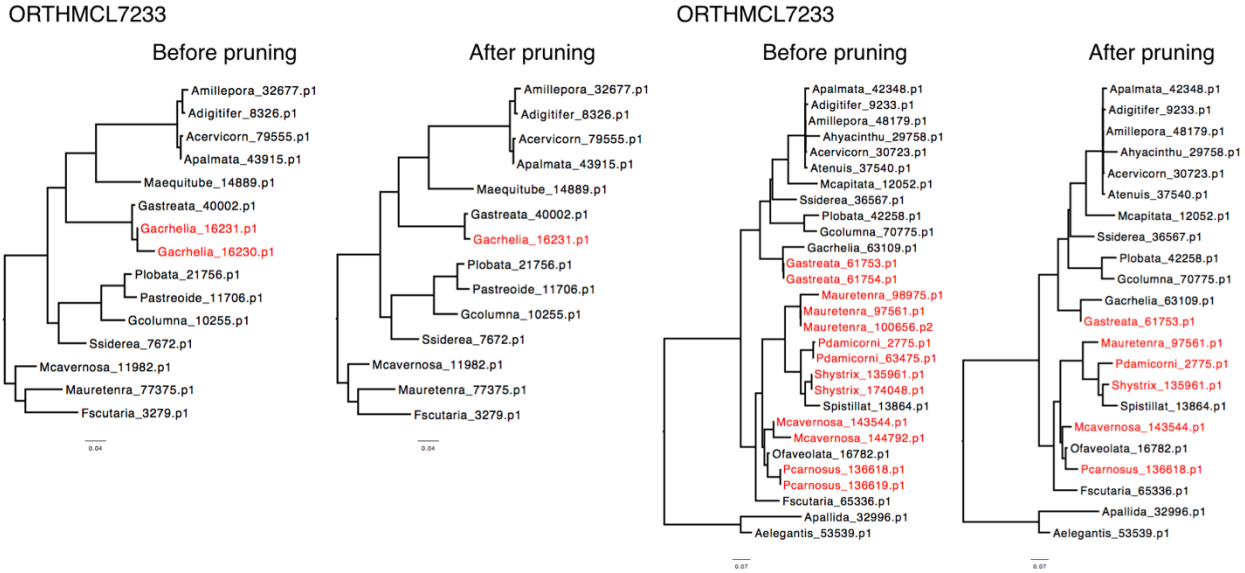

736

Figure S2: Categorization of all overlapping amino acid substitutions observed between all tested lineage pairs. An overlapping substitution is defined as an inferred amino acid change that occurred at the same position independently in the lineages leading to the common ancestor of the two indicated clades. To simplify comparisons, horizontal clades are labeled based on sisterhood to clades with vertical transmission (Fig. 1). Each overlapping substitution was classified into one of four categories: convergent substitutions (least frequent; salmon) are changes from different amino acids to the same amino acid; parallel substitutions (second most frequent; green) are changes from the same amino acid to the same new amino acid; divergent substitutions (most common; teal) are changes from the same amino acid to a different one; 'all different' substitutions (third most common; purple) are changes from different amino acids to different new amino acids. Examples of each type of overlapping substitution are show in in the legend.

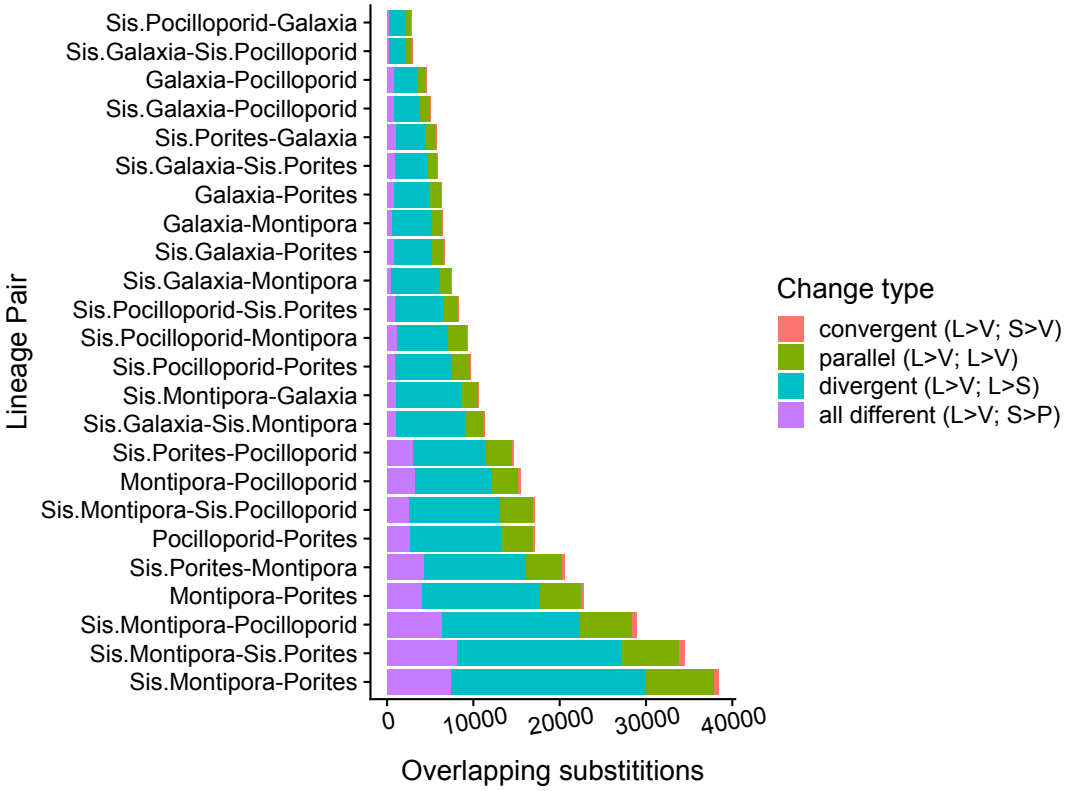

Figure S3: Comparison of frequency of convergent events among genes showing evidence of positive selection. (A) Counts of convergence events in genes showing evidence of positive selection in one or more of the indicated lineages. (B) Percentage of overlapping substitutions that were convergence events in genes also showing evidence of positive selection one or more of the indicated lineages. (C) Boxplot of the percentages in (B) split by phenotype pair, VV: vertical-vertical pairs, VH: vertical-horizontal pairs, HH: horizontal-horizontal pairs.

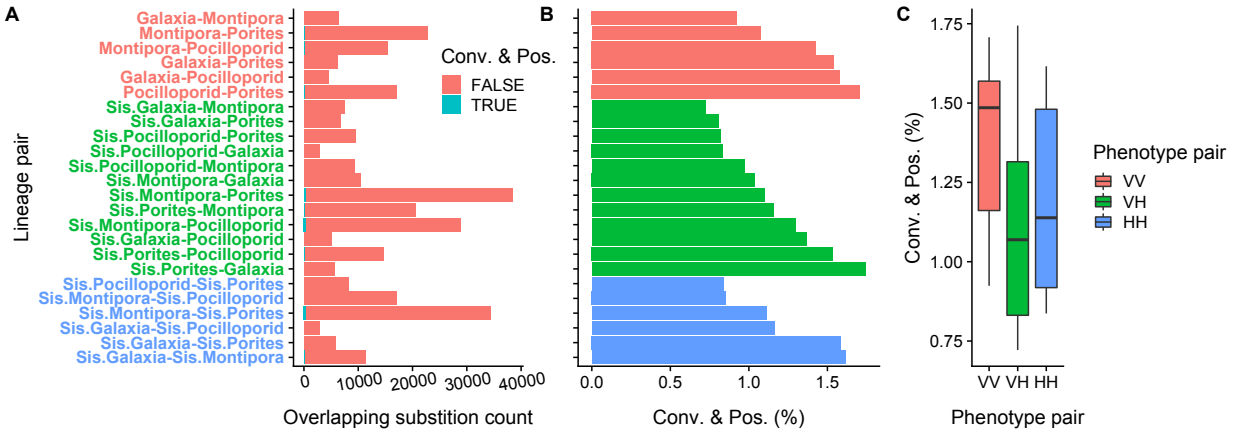

Figure S4: Comparison of the frequency of convergence events among overlapping substitutions. (A) Absolute counts of overlapping substitutions and convergence events for each species pair. (B) Percentage of overlapping substitutions that were convergence events. (C) Boxplot of the percentages in (B) split by phenotype pair, VV: vertical-vertical pairs, VH: vertical-horizontal pairs, HH: horizontal-horizontal pairs.

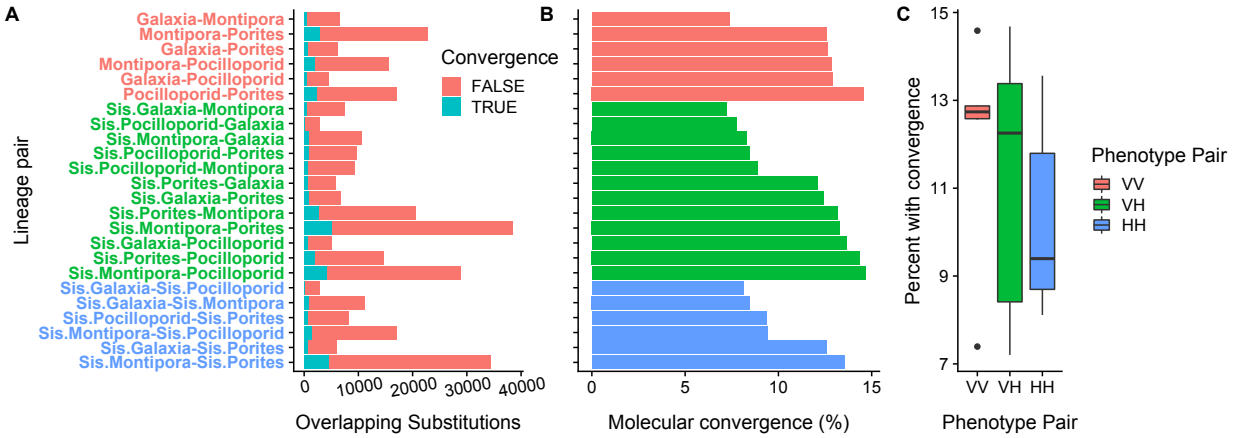

Figure S5: Comparison of the frequency of specific convergence events that were also identified as being positively selected. (A) Counts of convergence events which were also the sites exhibiting positive selection in one or more of the indicated lineages (Branch site test FDR < 0.1 for gene). (B) Percentage of overlapping substitutions that were convergence events in which the specific change was also the site of positive selection in one or more of the indicated lineages. Note that eight pairs have values of zero. (C) Boxplot of the percentages in (B) split by phenotype pair, VV: vertical-vertical pairs, VH: vertical-horizontal pairs, HH: horizontal-horizontal pairs.

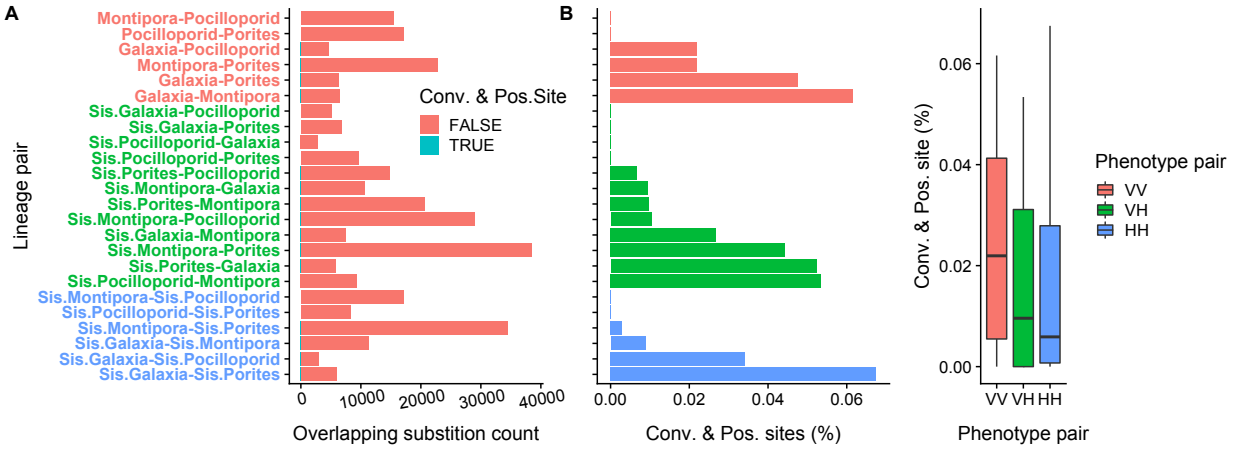

Figure S6: Functional enrichment for genes with convergence events and evidence of positive selection among horizontally transmitting sister clades. (A) Frequency of tested genes showing convergence and positive selection per pair of horizontally transmitting clades. Teal shading indicates the set of genes with at least one convergence event and evidence of positive selection (FDR < 0.1) in at least one of the indicated lineages. (B) Gene ontology enrichment across all convergent and positively selected genes identified for any pair of horizontally transmitting clades relative to the global gene list. Significance level is indicated by bolded text. Fractions preceding ontology terms indicate … (BP) Biological Processes, (CC) Cellular Component, (MF) Molecular Function. No ontology terms for Biological Process were significant.

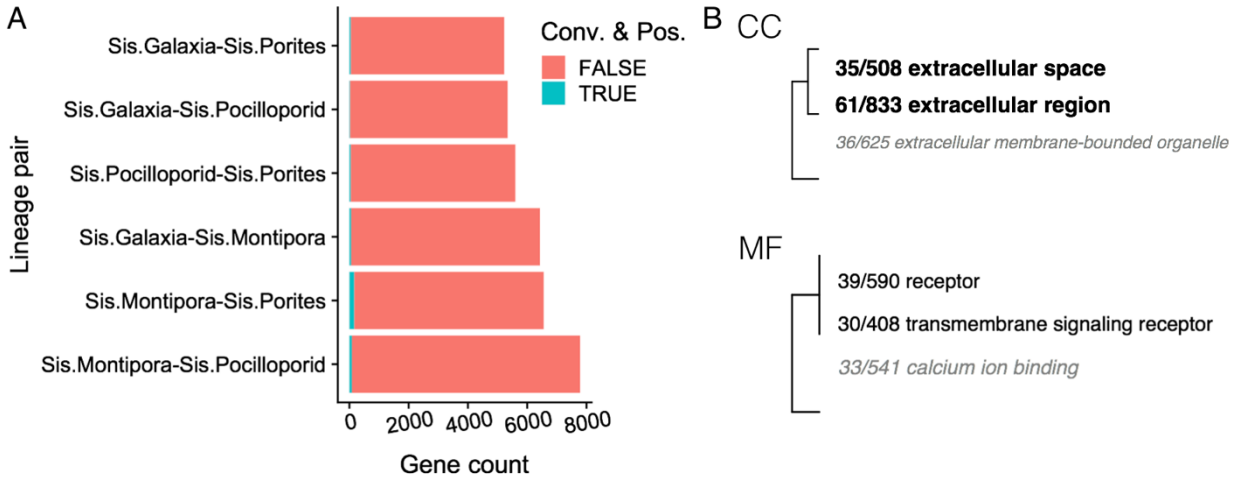

807 Figure S7: Labeling of branches for branch site tests. When performing the branch site test, the
808 branch or branches being tested for evidence of positive selection are labeled with "#1". When
809 testing for evidence of positive selection in a clade, we labeled only the branch leading to the
810 common ancestor of that clade. In cases when a clade had only a single species, for example
811 *Galaxia acrhelia*, the branch for that species was labeled.
812
813

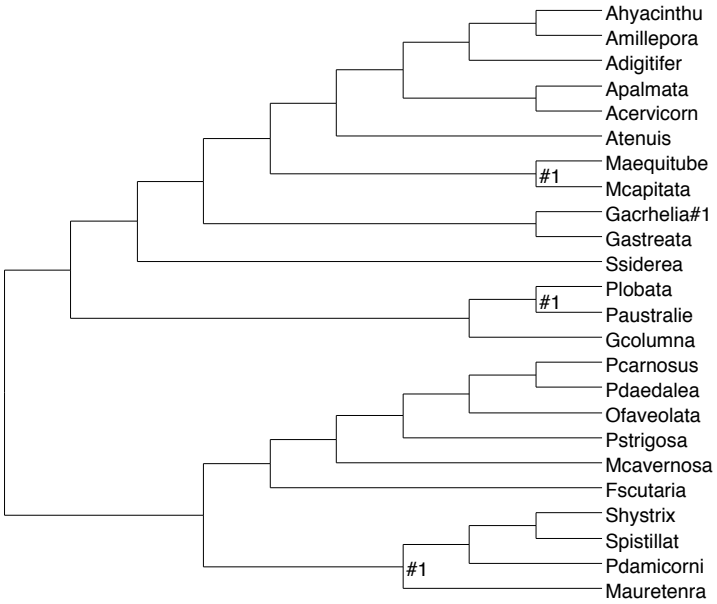

814
815
816